INT. J. CONTROL, 2004, VOL. 77, NO. 12, 1071–1082

Volterra series for solving weakly non-linear partial differential equations: application to a dissipative Burgers' equation

THOMAS HÉLIE†* and MARTIN HASLER‡

A method to solve weakly non-linear partial differential equations with Volterra series is presented in the context of single-input systems. The solution $x(z,t)$ is represented as the output of a z-parameterized Volterra system, where z denotes the space variable, but z could also have a different meaning or be a vector. In place of deriving the kernels from purely algebraic equations as for the standard case of ordinary differential systems, the problem turns into solving linear differential equations. This paper introduces the method on an example: a dissipative Burgers'equation which models the acoustic propagation and accounts for the dominant effects involved in brass musical instruments. The kernels are computed analytically in the Laplace domain. As a new result, writing the Volterra expansion for periodic inputs leads to the analytic resolution of the harmonic balance method which is frequently used in acoustics. Furthermore, the ability of the Volterra system to treat other signals constitutes an improvement for the sound synthesis. It allows the simulation for any regime, including attacks and transients. Numerical simulations are presented and their validity are discussed.

1. Introduction

Volterra series give a systematic representation for a wide class of non-linear systems, including linear differential systems, memory-less non-linear functions, and their combinations (Boyd 1985). Practically, they are very attractive for weakly non-linear ordinary differential equations for which keeping only the low-order kernels yields good approximations.

In this paper, the Volterra series are used in the more general context of a boundary controlled non-linear partial differential equation. Their formal framework gives an interesting alternative to the perturbation method usually used. The only difference with respect to the case of ordinary differential equations is the identification of the kernels: each one is performed by solving a linear differential rather than an algebraic equation.

The intended application deals with the acoustic propagation of planar waves in cylindrical ducts which induce visco-thermal losses on the wall. In such a case, the non-linearity of the propagation may lead to a shock-wave after a sufficiently long distance. For shorter distances, the weaker distortion is still audible for waves with high amplitudes, which is typical for brass instruments. Indeed, the so-called 'brass effect' exactly denotes the brightness of the sound obtained at *fortissimo*, due to this distortion.

The practical interest of using Volterra series is that the obtained input–output system allows the simulation of stationary waves as well as transients: standing waves or periodic inputs are not required as in the case of methods such as the harmonic balance (Menguy and Gilbert 2000).

This paper is structured as follows: In § 2, the investigated Burgers' acoustic model is presented and the Volterra series are briefly introduced, setting definitions, notations and describing useful properties.

Section 3 establishes the method used to solve the boundary controlled partial differential equation. The acoustic state is defined as the output of a Volterra system. The equations satisfied by the Volterra kernels are first derived. Second, their analytic resolution is performed, leading to a recursive relation. A clever decomposition which allows the numerical computation of the kernels and which can be generalized to the resolution of other problems is detailed.

In § 4, time simulations are presented for periodic signals and more generally for non-stationary signals. In the case of periodic signals, the analytic expressions of the kernels and the derivation of the Fourier coefficients of the output from those of the input give an analytic resolution of the harmonic balance. The validity of the results with respect to orders of approximation is quantified and physical interpretations are given.

Finally, before concluding, § 5 sketches limitations and extensions of the proposed method.

Received 2 December 2003. Revised 9 July 2004.
* Author for correspondence. e-mail: Thomas.Helie@lss.supelec.fr
†Laboratoire des Signaux et Systémes CNRS-Supélec-Université Paris-Sud, 3, rue Joliot Curie, F-91190 Gif-Sur-Yvette, France.
‡Laboratory of Nonlinear Systems (LANOS), Swiss Federal Institute of Technology, CH-1015 Lausanne, Switzerland.

International Journal of Control ISSN 0020–7179 print/ISSN 1366–5820 online © 2004 Taylor & Francis Ltd
http://www.tandf.co.uk/journals
DOI: 10.1080/00207170420002436

2. Problem statement

This section presents first the acoustic model of the propagation of progressive plane waves in a pipe, namely a dissipative Burgers' equation. This model is a non-linear partial differential equation which is valid for bounded amplitudes and frequencies such that the non-linearity of the model is weakly activated.

As weakly non-linear systems are well represented by Volterra series, the main idea of this paper is to solve the acoustic model thanks to this tool. This tool is introduced in the second part of this section.

2.1. *Model under study*

Let the massic density, the speed of the sound, the atmospheric pressure, the specific heat ratio, the kinematic viscosity, and the Prandtl number for the air be $\rho_0 \approx 1.2\,\mathrm{Kg\,m^{-3}}$, $c_0 \approx 344\,\mathrm{m\,s^{-1}}$, $P_0 \approx 1.013 \times 10^5\,\mathrm{Pa}$, $\gamma \approx 1.4$, $\nu \approx 1.5 \times 10^{-5}\,\mathrm{m^2\,s^{-1}}$ and $P_r \approx 0.7$, respectively.

In Menguy and Gilbert (2000), the acoustic waves propagating in a cylindrical pipe figure 1 are shown to be well described via two-dimensional progressive planar waves q^+ and q^- by

- massic density

$$\rho_a = \rho_0 \left[q^+ + q^- + O(M^2)\right] \tag{1}$$

- longitudinal particle velocity

$$u_a = c_0 \left[q^+ - q^- + O(M^2)\right] \tag{2}$$

- pressure

$$p_a = P_0\, \gamma \left[q^+ + q^- + O(M^2)\right] \tag{3}$$

where M denotes the order of magnitude of q^+, q^- and of the Mach number u_a/c_0.

These waves satisfy the generalized Burgers' equations

$$\xi\, \partial_\ell q \;=\; q\, \partial_\theta q \;-\; \alpha_0 \partial_\theta^{1/2} q \tag{4}$$

with $\xi = +1$ and $\theta = t - z/c_0$ for $q = q^+$, $\xi = -1$ and $\theta = t + z/c_0$ for $q = q^-$, and

$$\ell = \frac{1+\gamma}{2}\, z/c_0.$$

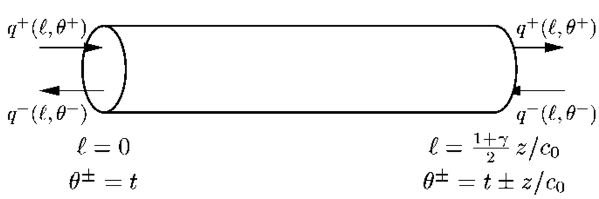

Figure 1. Progressive waves propagating in a cylindrical pipe.

The coefficient $\alpha_0 = (2/R_0)\,\kappa_0$ with

$$\kappa_0 = \frac{\sqrt{\nu}(\sqrt{P_r} + \gamma - 1)}{\sqrt{P_r}(\gamma + 1)} \approx 2.39 \times 10^{-3}\,\mathrm{m\,s^{-1/2}}$$

accounts for the visco-thermal losses for a pipe with radius R_0. The operator $\partial_\theta^{1/2}$ is the fractional derivative of order 1/2 for causal functions associated to the Laplace symbol $s^{1/2}$ on $\mathbb{C}$ with a cut on $\mathbb{R}^-$.

As the models for q^+ and q^- are symmetrical for $z \mapsto -z$, the problem is reduced without loss of generality to

$$\partial_\ell q \;=\; q\, \partial_\theta q \;-\; \alpha_0 \partial_\theta^{1/2} q. \tag{5}$$

The system defined in figure 1 and by (5) is weakly non-linear if $q\, \partial_\theta q$ is not greatly solicited. This occurs for small amplitudes and low frequencies, but also if this non-linearity is integrated over a short length, i.e. for small ℓ. For brass instruments, these features make the non-linearity weak but usually not negligible, so that Volterra series have a practical interest.

2.2. *Volterra series*

Only the principal definitions on the Volterra series and the relations used in this paper are recalled below. For a more detailed presentation see, e.g. Rugh (1981), Boyd (1985) and Hasler (1999).

2.2.1. *Definitions, notations and basic properties*. By definition, a system (**S**) is described by a Volterra series of kernels $\{h_n\}_{n \in \mathbb{N}^*}$ for inputs $|u(t)| < \rho$ if the output $y(t)$ is given by the multi-convolutions

$$y(t) = \sum_{n=1}^{+\infty} \iint_{-\infty}^{+\infty} h_n(\tau_1, \ldots, \tau_n) u(t - \tau_1) \ldots u(t - \tau_n)\, \mathrm{d}\tau_1 \ldots \mathrm{d}\tau_n. \tag{6}$$

Here, ρ is the convergence radius of $\sum_{n=1}^{+\infty} \|h_n\|_1 x^n$, with $\|h_n\|_1 = \iint_{-\infty}^{+\infty} |h_n(\tau_1, \ldots, \tau_n)|\, \mathrm{d}\tau_1 \ldots \mathrm{d}\tau_n$. For causal systems, h_n is zero for $\tau_k < 0$.

For causal systems, the mono-lateral Laplace transform of $h_n(\tau_1, \ldots, \tau_n)$ is denoted $H_n(s_1, \ldots, s_n)$ (Abramowitz and Stegun 1970, (29.1.2)). For s_k, $\mathrm{Re}(s_k) > 0$, H_n is analytic.

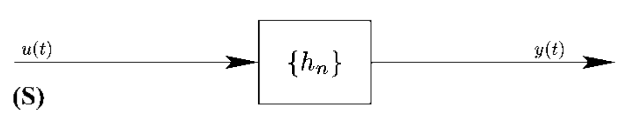

Figure 2. System (**S**) represented by Volterra kernels.

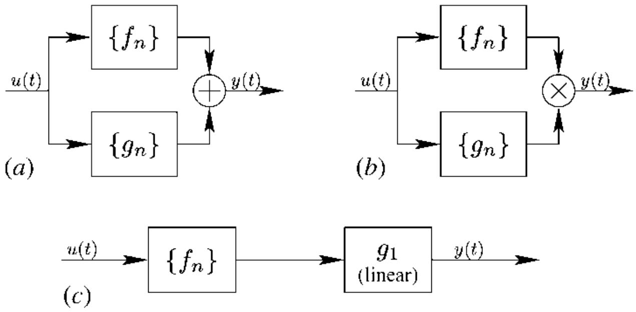

Figure 3. Sum (a), product (b), and cascade (c) of two systems.

2.3. *Interconnection laws*

The kernels $\{H_n\}$ of the systems (a), (b), and (c) in figure 3 are given respectively by (Hasler 1999, pp. 34, 35)

$$H_n(s_1, \ldots, s_n) = F_n(s_1, \ldots, s_n) + G_n(s_1, \ldots, s_n) \tag{7}$$

$$H_n(s_1, \ldots, s_n) = \sum_{p=1}^{n-1} F_p(s_1, \ldots, s_p)\, G_{n-p}(s_{p+1}, \ldots, s_n) \tag{8}$$

$$H_n(s_1, \ldots, s_n) = F_n(s_1, \ldots, s_n)\, G_1(s_1 + \cdots + s_n). \tag{9}$$

This paper is devoted to solving the acoustic problem using the Volterra series representation, and in particular, the relations (7)–(9) for the kernels. The method is now detailed.

3. Method and analytic computation of the kernels

This section introduces the method for computing the Volterra kernels of the system which generates the output $q(\ell, \theta)$ from the input $q(0, \theta)$. More precisely, the continuously space-parameterized state $q(\ell, \theta)$ is described as the output of a ℓ-parameterized Volterra system. It is well-known that in the case of ordinary differential equations, the Volterra kernels are obtained recursively by solving systems of linear algebraic equations in the Laplace domain. In the present case of partial differential equations, the kernels are parameterized by the spatial variable ℓ. It will be shown that they are obtained recursively by solving a linear differential equation (with respect to ℓ) in the Laplace domain (with respect to θ). The derivation of these equations is decribed in § 3.1.

Subsequently, the resolution of this equation is performed in § 3.2. It yields analytic expressions for the kernels in the form of a recursive formula which decomposes the solution on a set of exponentials.

Finally, in § 3.3, a more clever decomposition is obtained, which significantly simplifies the analytic computation of the kernels. This decomposition allows a straightforward implementation for numerical computations. Furthermore, it is well-adapted for extensions to other models and non-linearities.

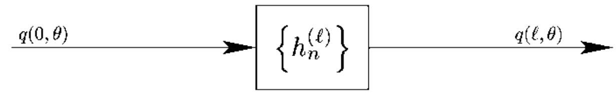

Figure 4. Definition of the Burgers' kernels.

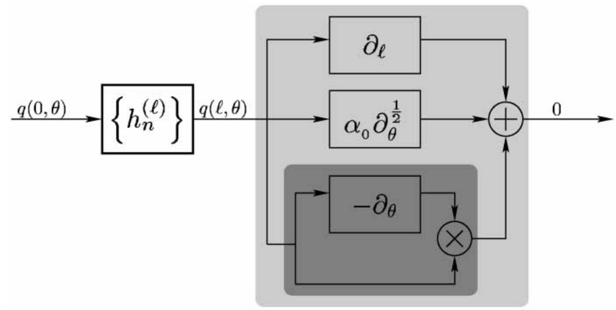

Figure 5. The output of the looked-for Volterra system representation are exactly those which make the output of the operator $X \mapsto Y = \partial_\ell X + \alpha_0 \partial_\theta^{1/2} X - X \partial_\theta X$ vanish (see (5)).

3.1. *Deriving the equations satisfied by the kernels*

Let the system (**S**) give the output $y^{(\ell)}(\theta) = q(\ell, \theta)$ from the input $u(\theta) = q(0, \theta)$ where q is governed by (5). Let $\{h_n^{(\ell)}(\theta_1, \ldots, \theta_n)\}_{n \in \mathbb{N}^*}$ be the ℓ-parameterized kernels of (**S**) (figure 4).

By definition, this system is the identity for $\ell = 0$ so that

$$H_1^{(0)}(s_1) = 1 \tag{10}$$

$$H_n^{(0)}(s_1, \ldots, s_n) = 0, \quad \forall n \geq 2. \tag{11}$$

Requiring that the Volterra kernels defines a system such that the outputs satisfy (5) is equivalent to imposing that the system represented in figure 5 is zero.

As the linear operator ∂_ℓ does not involve θ, the concatenation of the Volterra system with ∂_ℓ leads to the system (**S1**) defined by the kernels $\partial_\ell H_n^{(\ell)}(s_1, \ldots, s_n)$ in the Laplace domain. The operators ∂_θ and $\alpha_0 \partial_\theta^{1/2}$ are associated to the linear kernels $F_1(s) = s$ and $G_1(s) = \alpha_0 s^{1/2}$ respectively. The kernels of the Volterra system (**S2**) which generates the output of $\alpha_0 \partial_\theta^{1/2}$ are $\alpha_0 \sqrt{s_1 + \cdots + s_n}\, H_n^{(\ell)}(s_1, \ldots, s_n)$ from the interconnection law (9). Those of (**S3**) which generates the output of the non-linear part are $-\sum_{p=1}^{n-1}(s_1 + \cdots + s_p) \times H_p^{(\ell)}(s_1, \ldots, s_p) H_{n-p}^{(\ell)}(s_{p+1}, \ldots, s_n)$, from (8) and (9). Finally, writing that the cascade of systems depicted in figure 5 defines the null system is writing that the sum of the three systems (**S1**)+(**S2**)+(**S3**) is zero. From (9), this leads to

$$\partial_\ell H_n^{(\ell)}(s_1,\ldots,s_n) + \alpha_0\sqrt{s_1+\cdots+s_n}\, H_n^{(\ell)}(s_1,\ldots,s_n) = \sum_{p=1}^{n-1}(s_1+\cdots+s_p)\,H_p^{(\ell)}(s_1,\ldots,s_p)\,H_{n-p}^{(\ell)}(s_{p+1},\ldots,s_n) \tag{12}$$

which gives a linear ordinary differential equation to solve for each kernel $H_n^{(\ell)}$.

3.2. *Analytic solutions of the Volterra kernels*

Equations (10)–(12) make the resolution of the kernels possible, as described below.

3.2.1. *Linear kernel.* For $n=1$, equation (12) is

$$\partial_\ell H_1^{(\ell)}(s_1) + \alpha_0\sqrt{s_1}H_1^{(\ell)}(s_1) = 0 \tag{13}$$

so that the solution which satisfies (10) is

$$H_1^{(\ell)}(s_1) = \mathrm{e}^{-\alpha_0\ell\sqrt{s_1}}, \qquad \mathrm{Re}(s_1) > 0. \tag{14}$$

3.2.2. *Second order kernel.* For $n=2$, equation (12) becomes

$$\partial_\ell H_2^{(\ell)}(s_1,s_2) + \alpha_0\sqrt{s_1+s_2}H_2^{(\ell)}(s_1,s_2) = s_1\mathrm{e}^{-\alpha_0\ell(\sqrt{s_1}+\sqrt{s_2})}. \tag{15}$$

The solution which satisfies (11) is obtained

$$H_2^{(\ell)}(s_1,s_2) = \frac{s_1}{\alpha_0}\,\frac{\mathrm{e}^{-\alpha_0\ell\sqrt{s_1+s_2}} - \mathrm{e}^{-\alpha_0\ell(\sqrt{s_1}+\sqrt{s_2})}}{\sqrt{s_1}+\sqrt{s_2}-\sqrt{s_1+s_2}}. \tag{16}$$

3.2.3. *Higher order kernels.* By recurrence, it is proven in the next section that the kernels $H_n^{(\ell)}$ have the form

$$H_n^{(\ell)}(s_1,\ldots,s_n) = \sum P_i(s_1,\ldots,s_{n-1})\,\frac{\mathrm{e}^{-\alpha_0\ell\phi_i(s_1,\ldots,s_n)}}{A_i(s_1,\ldots,s_n)} \tag{17}$$

where P_i is a polynomial, $1/A_i$ is a rational function in square roots of sums of s_j, and ϕ_i is a sum of square roots of sums of s_j.

3.3. *Decomposition of the kernels*

Theorem: *The Volterra kernels are given by*

$$H_n^{(\ell)}(s_1,\ldots,s_n) = \sum_{\kappa\in\mathcal{K}_n} P_\kappa(s_1,\ldots,s_{n-1})f_\kappa^{(\ell)}(s_1,\ldots,s_n) \tag{18}$$

$$f_\kappa^{(\ell)}(s_1,\ldots,s_n) = \sum_{\lambda\in\Lambda_\kappa}\frac{\mathrm{e}^{-\alpha_0\ell\phi_\lambda(s_1,\ldots,s_n)}}{A_{\kappa,\lambda}(s_1,\ldots,s_n)} \tag{19}$$

where the sets of symbols $\mathcal{K}_n$ and Λ_κ and the functions P_κ ϕ_λ and $A_{\kappa,\lambda}$ are given by the following recursions:

(a) *The set of symbols $\mathcal{K}_1$ is composed of a single element which is arbitrarily denoted by ι*

$$\mathcal{K}_1 = \{\iota\}. \tag{20}$$

The set of symbols $\mathcal{K}_n$ is obtained by the recursion

$$\mathcal{K}_n = \bigcup_{p=1}^{n-1}\{\mathcal{K}_p\times\mathcal{K}_{n-p}\} \tag{21}$$

where '$\times$' is the cartesian product of sets. The symbols $\kappa_1\times(\kappa_2\times\kappa_3)$ and $(\kappa_1\times\kappa_2)\times\kappa_3$ are considered to be different.

(b) *The polynomial $P_\kappa(s_1,\ldots,s_{n-1})$, $\kappa\in\mathcal{K}_n$ is defined, for $n=1$, by*

$$P_\iota = 1 \tag{22}$$

and, for $n>1$, if $\kappa=\kappa_1\times\kappa_2$, with $\kappa\in\mathcal{K}_n$, $\kappa_1\in\mathcal{K}_p$, $\kappa_2\in\mathcal{K}_{n-p}$ by

$$P_\kappa(s_1,\ldots,s_{n-1}) = (s_1+\cdots+s_p)\times P_{\kappa_1}(s_1,\ldots,s_{p-1})\times P_{\kappa_2}(s_{p+1},\ldots,s_{n-1}). \tag{23}$$

(c) *The set Λ_κ, $\kappa\in\mathcal{K}_n$ is defined recursively, based on the sequence of arbitrary symbols w_i, $i=1,2,\ldots$, as follows. For $n=1$*

$$\Lambda_\iota = \{w_1\}. \tag{24}$$

For $n>1$, and $\kappa=\kappa_1\times\kappa_2$

$$\Lambda_\kappa = (\Lambda_{\kappa_1}\times\Lambda_{\kappa_2})\cup\{w_n\}. \tag{25}$$

(d) *The function ϕ_λ, $\lambda\in\Lambda_\kappa$, $\kappa\in\mathcal{K}_n$ is defined as follows. If $\lambda=w_n$*

$$\phi_{w_n}(s_1,\ldots,s_n) = \sqrt{s_1+\cdots+s_n} \tag{26}$$

and if $\lambda=\lambda_1\times\lambda_2$, corresponding to $\kappa=\kappa_1\times\kappa_2$, with $\kappa_1\in\mathcal{K}_p$, $\kappa_2\in\mathcal{K}_{n-p}$

$$\phi_\lambda(s_1,\ldots,s_n) = \phi_{\lambda_1}(s_1,\ldots,s_p)+\phi_{\lambda_2}(s_{p+1},\ldots,s_n). \tag{27}$$

(e) *The function $A_{\kappa,\lambda}$, $\lambda\in\Lambda_\kappa$, $\kappa\in\mathcal{K}_n$ is defined as follows. If $n=1$ and thus $\kappa=\iota$ and $\lambda=w_1$*

$$A_{\iota,w_1}(s_1) = 1. \tag{28}$$

If $n>1$, $\kappa=\kappa_1\times\kappa_2$, with $\kappa_1\in\mathcal{K}_p$, $\kappa_2\in\mathcal{K}_{n-p}$, and correspondingly $\lambda=\lambda_1\times\lambda_2$

$$A_{\kappa,\lambda}(s_1,\ldots,s_n) = -\alpha_0\,A_{\kappa_1,\lambda_2}(s_1,\ldots,s_p)\times A_{\kappa_1,\lambda_2}(s_{p+1},\ldots,s_n)[\phi_\lambda(s_1,\ldots,s_n)-\sqrt{s_1+\cdots+s_n}]. \tag{29}$$

Finally, if $n>1$ and $\lambda=w_n$

$$\frac{1}{A_{\kappa,w_n}(s_1,\ldots,s_n)} = -\sum_{\lambda\in\Lambda_\kappa\backslash\{w_n\}} \frac{1}{A_{\kappa,\lambda}(s_1,\ldots,s_p)}. \tag{30}$$

Proof (by recurrence)**:** For $n=1$, $\mathcal{K}_1=\{\iota\}$, $\Lambda_\iota=\{w_1\}$, and thus

$$H_1^{(\ell)}(s_1) = P_\iota \frac{\mathrm{e}^{-\alpha_0\ell\phi_{w_1}(s_1)}}{A_{\iota,w_1}(s_1)} = \mathrm{e}^{-\alpha_0\ell\sqrt{s_1}} \tag{31}$$

which coincides with (14).

Now, suppose the theorem is true for orders $1,\ldots,n-1$. The nth order Volterra kernel $H_n^{(\ell)}$ must satisfy the linear differential equation (12) in ℓ with initial condition (11). Its solution is

$$\begin{aligned}
&H_n^{(\ell)}(s_1,\ldots,s_n)\\
&=\sum_{p=1}^{n-1}(s_1+\cdots+s_p)\int_0^\ell \mathrm{e}^{-\alpha_0(\ell-x)\sqrt{s_1+\cdots+s_n}}\\
&\quad\times H_p^{(x)}(s_1,\ldots,s_p)H_{n-p}^{(x)}(s_{p+1},\ldots,s_n)\mathrm{d}x\\
&=\sum_{p=1}^{n-1}(s_1+\cdots+s_p)\int_0^\ell \mathrm{e}^{-\alpha_0(\ell-x)\sqrt{s_1+\cdots+s_n}}\\
&\quad\times\left[\sum_{\kappa_1\in\mathcal{K}_p}\sum_{\lambda_1\in\Lambda_{\kappa_1}} P_{\kappa_1}(s_1,\ldots,s_{p-1})\frac{\mathrm{e}^{-\alpha_0x\phi_{\lambda_1}(s_1,\ldots,s_p)}}{A_{\kappa_1,\lambda_1}(s_1,\ldots,s_p)}\right]\\
&\quad\times\left[\sum_{\kappa_2\in\mathcal{K}_{n-p}}\sum_{\lambda_2\in\Lambda_{\kappa_2}} P_{\kappa_2}(s_{p+1},\ldots,s_{n-1})\frac{\mathrm{e}^{-\alpha_0x\phi_{\lambda_2}(s_{p+1},\ldots,s_n)}}{A_{\kappa_2,\lambda_2}(s_{p+1},\ldots,s_n)}\right]\mathrm{d}x\\
&=\sum_{p=1}^{n-1}\sum_{\substack{\kappa_1\in\mathcal{K}_p\\ \kappa_2\in\mathcal{K}_{n-p}}}(s_1+\cdots+s_p)P_{\kappa_1}(s_1,\ldots,s_{p-1})P_{\kappa_2}(s_{p+1},\ldots,s_{n-1})\cdot\\
&\quad\times\sum_{\substack{\lambda_1\in\Lambda_{\kappa_1}\\ \lambda_2\in\Lambda_{\kappa_2}}}\frac{\int_0^\ell \mathrm{e}^{-\alpha_0(\ell-x)\sqrt{s_1+\cdots+s_n}-\alpha_0x(\phi_{\lambda_1}(s_1,\ldots,s_p)+\phi_{\lambda_2}(s_{p+1},\ldots,s_n))}\mathrm{d}x}{A_{\kappa_1,\lambda_1}(s_1,\ldots,s_p)A_{\kappa_2,\lambda_2}(s_{p+1},\ldots,s_n)}
\end{aligned} \tag{32}$$

$$\begin{aligned}
&=\sum_{p=1}^{n-1}\sum_{\substack{\kappa_1\in\mathcal{K}_p\\ \kappa_2\in\mathcal{K}_{n-p}}} P_{\kappa_1\times\kappa_2}(s_1,\ldots,s_{n-1})\\
&\quad\times\Bigg[\sum_{\substack{\lambda_1\in\Lambda_{\kappa_1}\\ \lambda_2\in\Lambda_{\kappa_2}}}\Big(\mathrm{e}^{-\alpha_0\ell(\phi_{\lambda_1}(s_1,\ldots,s_p)+\phi_{\lambda_2}(s_{p+1},\ldots,s_n))}\\
&\quad-\mathrm{e}^{-\alpha_0\ell\sqrt{s_1+\cdots+s_n}}\Big)\Big/\Big(-\alpha_0 A_{\kappa_1,\lambda_1}(s_1,\ldots,s_p)A_{\kappa_2,\lambda_2}(s_{p+1},\ldots,s_n)\\
&\quad\times\Big(\phi_{\lambda_1}(s_1,\ldots,s_p)+\phi_{\lambda_2}(s_{p+1},\ldots,s_n)-\sqrt{s_1+\cdots+s_n}\Big)\Big)\Bigg]\\
&=\sum_{\kappa\in\mathcal{K}_n}P_\kappa(s_1,\ldots,s_{n-1})\Bigg[\sum_{\lambda\in\Lambda_\kappa\backslash\{w_n\}}\frac{\mathrm{e}^{-\alpha_0\ell\phi_\lambda(s_1,\ldots,s_n)}}{A_{\kappa,\lambda}(s_1,\ldots,s_n)}\\
&\quad-\mathrm{e}^{-\alpha_0\ell\sqrt{s_1+\cdots+s_n}}\sum_{\lambda\in\Lambda_\kappa\backslash\{w_n\}}\frac{1}{A_{\kappa,\lambda}(s_1,\ldots,s_n)}\Bigg]\\
&=\sum_{\kappa\in\mathcal{K}_n}P_\kappa(s_1,\ldots,s_{n-1})\Bigg[\sum_{\lambda\in\Lambda_\kappa}\frac{\mathrm{e}^{-\alpha_0\ell\phi_\lambda(s_1,\ldots,s_n)}}{A_{\kappa,\lambda}(s_1,\ldots,s_n)}\Bigg]
\end{aligned} \tag{33}$$

which shows that $H_n^{(\ell)}$ has the form as stated in the theorem and thus concludes the proof. $\square$

3.4. *Computation of the three first kernels*

To get some feeling for the form of the various quantities, the explicit expressions are given for $n=2$ and $n=3$. The elements of the sets $\mathcal{K}_n$ and Λ_κ are enumerated according to the ordering defined by

$$\kappa_1\times(\kappa_2\times\kappa_3) < (\kappa_1\times\kappa_2)\times\kappa_3 \tag{34}$$

$$\lambda_1\times\lambda_2 < w_n \quad \text{if } \lambda_1\times\lambda_2\in\Lambda_\kappa \text{ and } w_n\in\Lambda_\kappa \tag{35}$$

The number of elements $K_n=\mathrm{card}(\mathcal{K}_n)$ of $\mathcal{K}_n$ is

$$K_1 = 1 \tag{36}$$

$$K_n=\sum_{p=1}^{n-1}K_p\,K_{n-p} \quad \text{for } n>1. \tag{37}$$

The ten first cardinals are $K_1=1$, $K_2=1$, $K_3=2$, $K_4=5$, $K_5=14$, $K_6=42$, $K_7=132$, $K_8=429$, $K_9=1430$ and $K_{10}=4862$. The number of elements $L_\kappa=\mathrm{card}(\Lambda_\kappa)$ of Λ_κ is

$$L_\iota = 1 \tag{38}$$

$$L_\kappa = 1+L_{\kappa_1}L_{\kappa_2} \quad \text{for } \kappa=\kappa_1\times\kappa_2. \tag{39}$$

For $n=1$, 2, 3, the corresponding L_κ are 1, 2, 3. For $n>3$, they no longer depend on the order n only, but on the index κ.

3.4.1. *Case* $n=2$.

$$\begin{aligned}
\mathcal{K}_2 &= \{\iota\times\iota\}\\
P_{\iota\times\iota}(s_1) &= s_1\\
\Lambda_{\iota\times\iota} &= \{w_1\times w_1, w_2\}\\
\phi_{w_1\times w_1} &= \sqrt{s_1}+\sqrt{s_2}\\
\phi_{w_2} &= \sqrt{s_1+s_2}\\
A_{\iota\times\iota,w_1\times w_1}(s_1,s_2) &= -\alpha_0(\sqrt{s_1}+\sqrt{s_2}-\sqrt{s_1+s_2})\\
A_{\iota\times\iota,w_2}(s_1,s_2) &= +\alpha_0(\sqrt{s_1}+\sqrt{s_2}-\sqrt{s_1+s_2}).
\end{aligned} \tag{40}$$

3.4.2. *Case* $n=3$.

$$\begin{aligned}
\mathcal{K}_3 &= \{\iota\times(\iota\times\iota), (\iota\times\iota)\times\iota\}\\
P_{\iota\times(\iota\times\iota)}(s_1,s_2) &= s_1\cdot s_2\\
P_{(\iota\times\iota)\times\iota}(s_1,s_2) &= s_1\,(s_1+s_2)
\end{aligned} \tag{41}$$

$$\begin{aligned}
\Lambda_{\iota\times(\iota\times\iota)} &= \{w_1\times(w_1\times w_1), w_1\times w_2, w_3\}\\
\Lambda_{(\iota\times\iota)\times\iota} &= \{(w_1\times w_1)\times w_1, w_2\times w_1, w_3\}
\end{aligned} \tag{42}$$

$$\begin{aligned}\phi_{w_1\times w_1\times w_1} &= \sqrt{s_1}+\sqrt{s_2}+\sqrt{s_3}\\ \phi_{w_1\times w_2} &= \sqrt{s_1}+\sqrt{s_2+s_3}\\ \phi_{w_2\times w_1} &= \sqrt{s_1+s_2}+\sqrt{s_3}\\ \phi_{w_3} &= \sqrt{s_1+s_2+s_3}.\end{aligned}\tag{43}$$

Note that for functions ϕ_λ, the symbols $(\lambda_1\times\lambda_2)\times\lambda_3$ and $\lambda_1\times(\lambda_2\times\lambda_3)$ do not require to be distinguished. Morevover, the word $w_{k_1}\times\cdots\times w_{k_m}$ can be understood as follows. The symbol w_k indicates that k variables s_p are consecutively added under a square-root, while $\times$ corresponds to a consecutive addition outside the square root.

$$\begin{aligned}A_{\iota\times(\iota\times\iota),w_1\times(w_1\times w_1)} &= \alpha_0^2\big(\sqrt{s_2}+\sqrt{s_3}-\sqrt{s_2+s_3}\big)\\ &\quad\times\big(\sqrt{s_1}+\sqrt{s_2}+\sqrt{s_3}-\sqrt{s_1+s_2+s_3}\big)\\ A_{\iota\times(\iota\times\iota),w_1\times w_2} &= -\alpha_0^2\big(\sqrt{s_2}+\sqrt{s_3}-\sqrt{s_2+s_3}\big)\\ &\quad\times\big(\sqrt{s_1}+\sqrt{s_2+s_3}-\sqrt{s_1+s_2+s_3}\big)\\ A_{\iota\times(\iota\times\iota),w_3} &= \alpha_0^2\big(\sqrt{s_1}+\sqrt{s_2}+\sqrt{s_3}-\sqrt{s_1+s_2+s_3}\big)\\ &\quad\times\big(\sqrt{s_1}+\sqrt{s_2+s_3}-\sqrt{s_1+s_2+s_3}\big)\\ A_{(\iota\times\iota)\times\iota,(w_1\times w_1)\times w_1} &= \alpha_0^2\big(\sqrt{s_1}+\sqrt{s_2}-\sqrt{s_1+s_2}\big)\\ &\quad\times\big(\sqrt{s_1}+\sqrt{s_2}+\sqrt{s_3}-\sqrt{s_1+s_2+s_3}\big)\end{aligned}\tag{44}$$

$$\begin{aligned}A_{(\iota\times\iota)\times\iota,w_2\times w_1} &= -\alpha_0^2\big(\sqrt{s_1}+\sqrt{s_2}-\sqrt{s_1+s_2}\big)\\ &\quad\times\big(\sqrt{s_1+s_2}+\sqrt{s_3}-\sqrt{s_1+s_2+s_3}\big)\\ A_{(\iota\times\iota)\times\iota,w_3} &= A_{\iota\times(\iota\times\iota),w_3}\\ &= \alpha_0^2\big(\sqrt{s_1}+\sqrt{s_2}+\sqrt{s_3}-\sqrt{s_1+s_2+s_3}\big)\\ &\quad\times\big(\sqrt{s_1}+\sqrt{s_2+s_3}-\sqrt{s_1+s_2+s_3}\big).\end{aligned}$$

3.5. *Analytic continuation and singular terms*

A priori, the frequency domain kernels are well defined in the cartesian product of the right half complex planes, i.e. for the frequency points $\boldsymbol{s}=(s_1,\ldots,s_n)$ with $\mathrm{Re}(s_i)>0$. However, by analytic continuation, they can be defined for each frequency as holomorphic functions in the whole complex plane, excluding the negative real axis $(\mathbb{C}\backslash\mathbb{R}^-)^n$. This can be seen as follows. For $n=1$, expression (31) implies the fact. The higher-order kernels are determined from the lower-order kernels by the solution of the linear differential equation (29), given in (33). Thus, from the analytic continuation of the lower-order kernels, we obtain the analytic continuation of the higher-order kernels.

In the decomposition (19) of the kernels, the denominators $A_{\kappa,\lambda}$ vanish at certain combinations of frequencies and thus the kernels cannot be evaluated numerically at these frequency vectors by following the recursive computation described in the theorem, as it stands. On the other hand, the kernels themselves have no singularity outside when no frequency is negative real. Therefore, the singularities of the various terms must cancel. Indeed, this can be seen explicitly as follows. Suppose that for some vector $\boldsymbol{s}^\dagger=(s_1^\dagger,\ldots,s_n^\dagger)$, and some $\lambda=\lambda_1\times\lambda_2\in\Lambda_\kappa$, $\kappa\in\mathcal{K}_n$

$$\phi_\lambda(s_1^\dagger,\ldots,s_n^\dagger)=\sqrt{s_1^\dagger+\cdots+s_n^\dagger}.\tag{45}$$

Then, the term

$$P_\kappa(s_1,\ldots,s_{n-1})\frac{\mathrm{e}^{-\alpha_0\ell\phi_\lambda(s_1,\ldots,s_n)}}{A_{\kappa,\lambda}(s_1+\cdots+s_n)}$$

of the kernel $H_n^{(\ell)}(s_1,\ldots,s_n)$ is singular at $\boldsymbol{s}^\dagger$ because of the factor $\phi_\lambda(s_1,\ldots,s_n)-\sqrt{s_1+\cdots+s_n}$ in $A_{\kappa,\lambda}(s_1,\ldots,s_n)$ (cf. (29)). On the other hand, the term

$$P_\kappa(s_1,\ldots,s_{n-1})\frac{\mathrm{e}^{-\alpha_0\ell\sqrt{s_1+\cdots+s_n}}}{A_{\kappa,w_n}(s_1,\ldots,s_n)}$$

contains the same factor, and thanks to (30), we can write

$$\begin{aligned}&\frac{\mathrm{e}^{-\alpha_0\ell\phi_\lambda(s_1,\ldots,s_n)}}{A_{\kappa,\lambda}(s_1,\ldots,s_n)}-\frac{\mathrm{e}^{-\alpha_0\ell\sqrt{s_1+\cdots+s_n}}}{A_{\kappa,w_n}(s_1,\ldots,s_n)}\\ &\quad=\frac{\mathrm{e}^{-\alpha_0\ell\phi_\lambda(s_1,\ldots,s_n)}-\mathrm{e}^{-\alpha_0\ell\sqrt{s_1+\cdots+s_n}}}{A_{\kappa,\lambda}(s_1,\ldots,s_n)}\\ &\quad-\sum_{\lambda'\in\Lambda_\kappa\backslash\{w_n,\lambda\}}\frac{\mathrm{e}^{-\alpha_0\ell\sqrt{s_1+\cdots+s_n}}}{A_{\kappa,\lambda'}(s_1+\cdots+s_n)}\\ &=\frac{\mathrm{e}^{-\alpha_0\ell\phi_\lambda(s_1,\ldots,s_n)}}{A_{\kappa,\lambda}(s_1,\ldots,s_n)}\frac{1-\mathrm{e}^{-\alpha_0\ell[\sqrt{s_1,\ldots,s_n}-\phi_\lambda(s_1,\ldots,s_n)]}}{\sqrt{s_1,\ldots,s_n}-\phi_\lambda(s_1,\ldots,s_n)}\\ &\quad-\sum_{\lambda'\in\Lambda_\kappa\backslash\{w_n,\lambda\}}\frac{\mathrm{e}^{-\alpha_0\ell\sqrt{s_1+\cdots+s_n}}}{A_{\kappa,\lambda'}(s_1,\ldots,s_n)}\end{aligned}\tag{46}$$

At $\boldsymbol{s}=\boldsymbol{s}^\dagger$, this expression has the finite value

$$\frac{\mathrm{e}^{-\alpha_0\ell\phi_\lambda(s_1,\ldots,s_n)}}{A_{\kappa,\lambda}(s_1,\ldots,s_n)}\alpha_0\ell-\sum_{\lambda'\in\Lambda_\kappa\backslash\{w_n,\lambda\}}\frac{\mathrm{e}^{-\alpha_0\ell\sqrt{s_1+\cdots+s_n}}}{A_{\kappa,\lambda'}(s_1,\ldots,s_n)}.\tag{47}$$

Accordingly, the recursive determination (29) and (30) of $A_{\kappa,\lambda}(s_1,\ldots,s_n)$ has to be completed by the

complement:

For those values of $(s_1,\ldots,s_n)$ for which

$$\phi_\lambda(s_1,\ldots,s_n)=\sqrt{s_1+\cdots+s_n}\tag{48}$$

where $\lambda = \lambda_1 \times \lambda_2 \in \Lambda_\kappa$, $\kappa \in \mathcal{K}_n$, the value of $A_{\kappa,\lambda}(s_1, \ldots, s_n)$ becomes a function of ℓ and is determined by

$$A^{(\ell)}_{\kappa,\lambda}(s_1, \ldots, s_n) = -\frac{1}{\ell} A_{\kappa_1,\lambda_1}(s_1, \ldots, s_p) A_{\kappa_2,\lambda_2}(s_{p+1}, \ldots, s_n) \tag{49}$$

and $A_{\kappa, w_n}(s_1, \ldots, s_n)$ by

$$\frac{1}{A_{\kappa, w_n}(s_1, \ldots, s_n)} = -\sum_{\lambda \in \Lambda_\kappa \setminus \{w_n, \lambda_1 \times \lambda_2\}} \frac{1}{A_{\kappa,\lambda}(s_1, \ldots, s_p)}. \tag{50}$$

Note that for a degenerecence of higher order, i.e. when (48) holds but A_{κ_1,λ_1} or A_{κ_1,λ_1} depend on ℓ because of a previous degenerescence, similar relations can be carried out, which still make the numerical evaluation of the corresponding kernels possible. They lead to functions $1/A^{(\ell)}_{\kappa,\lambda}$ which are polynomials in ℓ.

4. Numerical results and physical interpretations

4.1. *Periodic signals*

4.1.1. *An analytic resolution of the harmonic balance*. The harmonic balance is a method which determines periodic dynamics of non-linear systems by computing the Fourier coefficients up to a fixed order of approximation. This standard method relies on an iterative algorithm which makes the coefficients converge towards the solution (see Nakhla and Vlach (1976) for a full description of the method). Here, the analytic expressions of the Volterra kernels allow us to build a non-iterative resolution of this problem. The method is given by well-known relations: for a periodic signal $u(\theta) = \sum_{k=-\infty}^{+\infty} c_k\, e^{ik\omega\theta}$, the response of the system takes the particular form $y(\theta) = \sum_{k=-\infty}^{+\infty} d_k\, e^{ik\omega\theta}$ where (Hasler 1999, (3.104))

$$d_k = \sum_{n=1}^{+\infty} \sum_{\substack{k_1,\ldots,k_n=-\infty \\ k_1+\cdots+k_n=k}}^{+\infty} c_{k_1} \ldots c_{k_n} H_n(ik_1\omega, \ldots, ik_n\omega). \tag{51}$$

For real input signals and systems, the hermitian symmetries $c_{-k} = \overline{c_k}$ and $d_{-k} = \overline{d_k}$ yield $u(\theta) = 2\,\mathrm{Re}\big(\sum_{k=0}^{+\infty} c_k\, e^{ik\omega\theta}\big)$ and $y(\theta) = 2\,\mathrm{Re}\big(\sum_{k=0}^{+\infty} d_k\, e^{ik\omega\theta}\big)$.

4.1.2. *Example for a sinusoidal input*. The analytic computation of d_k is detailed for a sinusoidal input signal and considering the non-linearity up to both the second and the third order.

The input signal is $u(\theta) = a\cos(\omega\theta)$ ($c_1 = c_{-1} = a/2$ and $c_k = 0$ else) and the pipe is represented by the kernels $\{H_1, H_2\}$. This yields an output which is the sum of a constant, a fundamental (ω), and a second harmonic (2ω) components. The constant term is

$$d_0 = c_{-1} c_1 \Big[H_2^{(\ell)}(i\omega, -i\omega) + H_2^{(\ell)}(-i\omega, i\omega)\Big] = 0. \tag{52}$$

The fundamental component is

$$\begin{aligned} d_{-1}\, e^{-i\omega\theta} + d_1\, e^{i\omega\theta} &= c_{-1} H_1^{(\ell)}(-i\omega)\, e^{-i\omega\theta} + c_1 H_1^{(\ell)}(i\omega)\, e^{i\omega\theta} \\ &= a\, e^{-\alpha_0 \ell \sqrt{\omega/2}} \cos\Big(\omega\theta - \alpha_0 \ell \sqrt{\frac{\omega}{2}}\Big). \end{aligned} \tag{53}$$

The second harmonic component is

$$\begin{aligned} & d_{-2}\, e^{-2i\omega\theta} + d_2\, e^{2i\omega\theta} \\ &= c_{-1}^2 H_2^{(\ell)}(-i\omega, -i\omega) e^{-2i\omega\theta} \\ &\quad + c_1^2 H_2^{(\ell)}(i\omega, i\omega)\, e^{2i\omega\theta} \\ &= \frac{a^2\sqrt{\omega}}{2\alpha_0(2-\sqrt{2})} \Big[e^{-\alpha_0\ell\sqrt{\omega}} \cos\Big(2\omega\theta - \alpha_0\ell\sqrt{\omega} + \frac{\pi}{4}\Big) \\ &\quad - e^{-\alpha_0\ell\sqrt{2\omega}} \cos\Big(2\omega\theta - \alpha_0\ell\sqrt{2\omega} + \frac{\pi}{4}\Big)\Big]. \end{aligned} \tag{54}$$

For higher amplitudes, higher-order non-linearities of the system are activated, requiring to increase the order of approximations (quantitative estimations are given below). Considering the Volterra kernels up to the third order leads to the Fourier coefficients

$$d_0 = \Big(\frac{a}{2}\Big)^2 [H_2(i\omega, -i\omega) + H_2(-i\omega, i\omega)] = 0 \tag{55}$$

$$\begin{aligned} d_1 &= \frac{a}{2} H_1(i\omega) + \Big(\frac{a}{2}\Big)^3 \big[H_3(i\omega, i\omega, -i\omega) + H_3(i\omega, -i\omega, i\omega) \\ &\quad + H_3(-i\omega, i\omega, i\omega)\big] \\ &= \frac{a}{2}\, e^{-\alpha_0\ell\sqrt{i\omega}} + \Big(\frac{a}{2}\Big)^3 \frac{i\omega}{\alpha_0^2(2-\sqrt{2})} \\ &\quad \times \left[\frac{e^{-\alpha_0\ell(2-i)\sqrt{i\omega}} - e^{-\alpha_0\ell\sqrt{i\omega}}}{1-i} - \frac{e^{-\alpha_0\ell(\sqrt{2}-i)\sqrt{i\omega}} - e^{-\alpha_0\ell\sqrt{i\omega}}}{\sqrt{2}-1-i} \right] \end{aligned} \tag{56}$$

$$\begin{aligned} d_2 &= \Big(\frac{a}{2}\Big)^2 H_2(i\omega, i\omega) \\ &= \Big(\frac{a}{2}\Big)^2 \frac{\sqrt{i\omega}}{\alpha_0(2-\sqrt{2})} \Big[e^{-\alpha_0\ell 2\sqrt{i\omega}} - e^{-\alpha_0\ell\sqrt{2i\omega}} \Big] \end{aligned} \tag{57}$$

$$\begin{aligned} d_3 &= \Big(\frac{a}{2}\Big)^3 H_3(i\omega, i\omega, i\omega) \\ &= \Big(\frac{a}{2}\Big)^3 \frac{3i\omega}{\alpha_0^2(2-\sqrt{2})} \left[\frac{e^{-\alpha_0\ell 3\sqrt{i\omega}} - e^{-\alpha_0\ell\sqrt{3i\omega}}}{3-\sqrt{3}} \right. \\ &\quad \left. - \frac{e^{-\alpha_0\ell(1+\sqrt{2})\sqrt{i\omega}} - e^{-\alpha_0\ell\sqrt{3i\omega}}}{1+\sqrt{2}-\sqrt{3}} \right] \end{aligned} \tag{58}$$

$d_k = 0$ for $k \geq 4$ and $d_{-k} = \overline{d_k}$. Then, the output has the analytic expression $y(\theta) = 2\,\mathrm{Re}\big[\sum_{k=1}^{3} d_k\, e^{ik\omega\theta}\big]$, which is not expanded for sake of conciseness.

Over and above the expected creation of a third harmonic, another effect of the third order kernel is the modification of the fundamental component. This

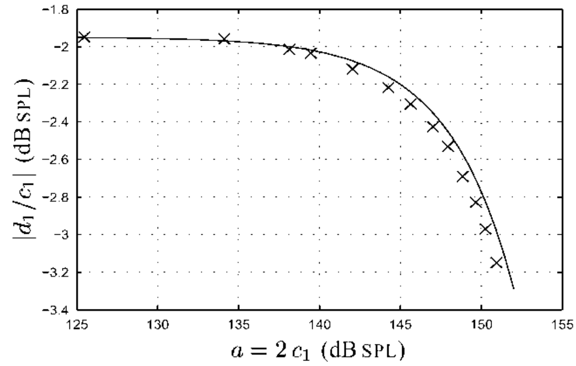

Figure 6. The ratio $|d_1/c_1|$ of the fundamental amplitude of the output ($L = 4.98$ m) over that of the input is plotted with respect to $a = 2\,c_1$. The parameters of the experiment are $F = 2$ kHz, $R_0 = 29$ mm, $L = 4.98$ m. As $\alpha_0 = 0.164$ and $\gamma = 1.4$ are reliable parameters (see § 2.1), the speed of the sound which depends of the temperature, is determined from the first measure. It is deduced from the attenuation modeled by $|H_1 i\omega|$ since the linear propagation is available at 125 dB SPL. The estimation is $c_0 = 347\,\mathrm{m\,s^{-1}}$. Experiments ($\times$) and the analytic determination (–) from the the first three Volterra kernels are quite in agreements. These experimental data have been extracted from Menguy and Gilbert (2000, figure 3*a*, curve (3)).

effect has been experimentally measured in Menguy and Gilbert (2000) and is compared in figure 6. A good agreement is observed, although the third-order approximation is the coarsest one which can model such a variation.

Results of simulations with $\{H_{n=1,2,3,4}\}$ are given in figure 7 for various length of pipes. No qualitative differences are observed for $\ell_{k=1,2,3}$ when considering $N=2$ or $N=3$ as the order of approximation in place of $N=4$.

4.1.3. *Radius of convergence and ideal order of approximation.* The analytic computation of the radius of convergence of the Volterra series has not been performed. Indeed, determining the kernels in the time domain to evaluate their infinite norms make some

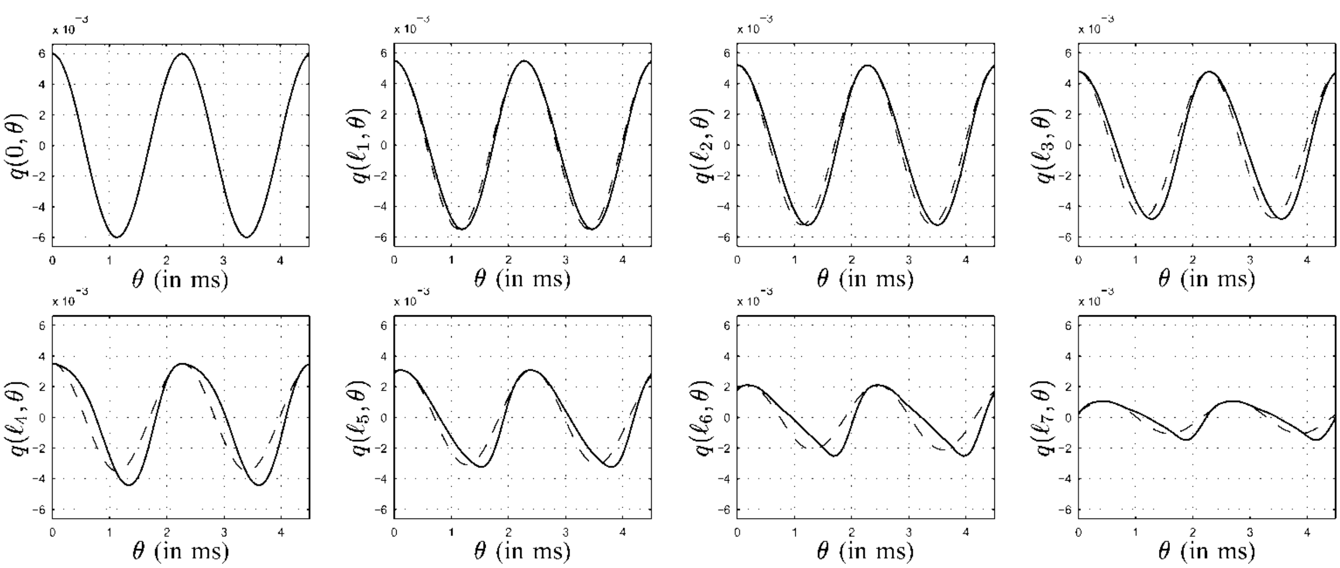

Figure 7. The output (–) of the system is computed considering the kernels $H_{n=1,2,3,4}$ for a sinusoidal input with $a = 6e-3 \equiv 152.6$ dB SPL, $F = 440$ Hz, $\alpha_0 = 4.77e-1$ (i.e. a pipe of radius $R_0 = 1$ cm), and for $\ell_0 = 0$, $\ell_1 = 4.95e-3$, $\ell_2 = 7.88e-3$, $\ell_3 = 1.26e-2$, $\ell_4 = 2.25e-2$, $\ell_5 = 3.58e-2$, $\ell_6 = 5.7e-2$, and $\ell_7 = 9.08e-2$. These dimensionless lengths correspond respectively to $L = 0$ m, 1.41 m, 2.26 m, 3.6 m, 6.44 m, 10.26 m, 16.34 m and 26 m. In order to appreciate the waveforms, the sinusoid which takes the same maximal value at the same θ than $q(\ell,\theta)$ is represented with dashed lines.

complications appear in the calculus. Nevertheless, an idea of this radius can be obtained through an estimation computed directly in the Fourier domain.

If a Volterra series has a radius of convergence ρ, the kernels H_n asymptotically satisfy the relation (Hasler 1999, p. 51)

$$\left|H_n(i\omega_1,\ldots,i\omega_n)\right| \sim \frac{\beta}{\rho^n} \tag{59}$$

where β is a constant. In this case, an estimation for the sinusoidal case presented above is given by (see figure 8(a, b))

$$\rho \sim \rho_n = \left|H_n(i\omega,\ldots,i\omega)/H_{n+1}(i\omega,\ldots,i\omega)\right| \tag{60}$$

asymptotically. As expected (figure 8(*b*)), this radius is infinite for $\ell = 0$ since identity is linear.

From a numerical point of view, a crucial decision concerns the evaluation of a required order of approximation: how many kernels may be taken into account to ensures the validity of the result? Inside the convergence disc, an estimation of the N-order remainder of the series can be approximated by

$$R_n = \left|\beta \frac{(a/\rho)^n}{1-(a/\rho)}\right|. \tag{61}$$

Moreover, the Burgers' generalized model (5) ensures errors of order $\mathcal{O}(a^2)$ on the output signal [see (1)–(3)]. As a consequence, it is useless to overstep the order N^* such that $R_{N^*} = a^2$. The determination of such an order is illutrated in figure 8(*c*).

4.1.4. *Remark on quasi-periodic signals*. As for the standard harmonic balance, an extension to quasi-periodic signals is possible. The analytic expression of $y(\theta)$ for a given set of non-commensurable frequencies also exists [see Hasler 1999, (3.119) for details].

4.2. *Discrete time simulation for non-stationary signals*

The main interest of Volterra series for time simulation is that it is not limited to periodic, quasi-periodic, nor stationary signals. This is a crucial point for most of applications, including sound synthesis. Another interesting feature from a signal processing point of view concerns the control of aliasing. For an approximation of order N, the Shannon–Nyquist theorem guarantees that no aliasing occurs taking a sampling frequency F_s greater than $2NF_{\max}$ where $F_{\max}$ denotes the highest frequency that the input signal contains.

Thus, making use of a discrete implementation of the multi-convolution (6) yields an algorithm. The kernels in the time domain $\{h_1^{(\ell)}(\theta_1),\ldots,h_N^{(\ell)}(\theta_1,\ldots,\theta_N\}$ can be computed from the multi-dimensional inverse discrete Fourier transform of $\{H_1^{(\ell)}(i\omega_1),\ldots,h_N^{(\ell)}(i\omega_1,\ldots,i\omega_n\}$. As a particular case, $h_1^{(\ell)}(\theta_1)$ can be derived analytically (Abramowitz and Stegun (1970, (29.3.82))

$$h_1^{(\ell)}(\theta_1) = \frac{\alpha_0\,\ell}{2\sqrt{\pi\theta_1^3}}\,\mathrm{e}^{-\alpha_0^2\ell^2/4\theta_1}\,\mathbf{1}_{\theta_1>0}(\theta_1). \tag{62}$$

Another algorithm is obtained making use of the discrete inverse Fourier Transform to implement the computation of [Hasler 1999, (3.123)]

$$y(\theta) = \sum_{n=1}^{+\infty}\int_{R^n} U(\omega_1)\ldots U(\omega_n) \times H_n(i\omega_1,\ldots,i\omega_n)\mathrm{e}^{i(\omega_1+\cdots+\omega_n)\theta}\,\mathrm{d}\omega_1\ldots\mathrm{d}\omega_n, \tag{63}$$

which uses the frequency domain version of (6) and where $U(\omega)$ denotes the Fourier transform of $u(\theta)$.

Such methods have a very high cost of computation due to the multi-dimensional convolutions (6) and multi-dimensional inverse Fourier transforms (63), respectively. For this reason, the following example is computed only for $N=2$. To build an example of a musical application, the pipe is defined for $R_0 = 5.6$ mm and $L = 4$ m, so that $\alpha_0 = 0.852$ and $\ell = 1.4e-2$, and where R_0 is typical of a brass musical instrument. The input signal $u(\theta)$ has the main features of a "musical note" (an attack, a sustain, a decay, a vibrato) and is described by

$$u(\theta) = A(\theta)\sin\left(2\pi\int_0^\theta f(\tau)\,\mathrm{d}\tau\right) \tag{64}$$

where the amplitude A and and the frequency f are given by $A(\theta) = a\,\theta/\theta_1$ for $0 \le \theta \le \theta_1$, $A(\theta) = a$ for $\theta_1 \le \theta \le \theta_2$, $A(\theta) = a\left(1-(\theta-\theta_2)/(\theta_3-\theta_2)\right)$ for $\theta_2 \le \theta \le \theta_3$, and $f(\theta) = F_0 + \Delta_F\sin(2\pi F_{\mathrm{vib}}\theta)$. In order to exhibit the progressive activation of the non-linearity, a smooth attack is chosen with $\theta_1 = 150$ ms. Other parameters are $a = 4.8e-3 \equiv 150.6$ dB SPL so that $N^* = 3$, $\theta_2 = 100$ ms, $\theta_3 = 500$ ms, $F_0 = 440$ Hz, $\Delta_F = 22$ Hz, and $F_{\mathrm{vib}} = 5$ Hz. The spectrograms of the input and the output are given in figure 9.

The simulations yield satisfying features, mainly:

- the output signal is damped because of the visco-thermal losses;
- the 'non-stationnary' second harmonic is created which coincides with the frequency $2f(\theta)$;

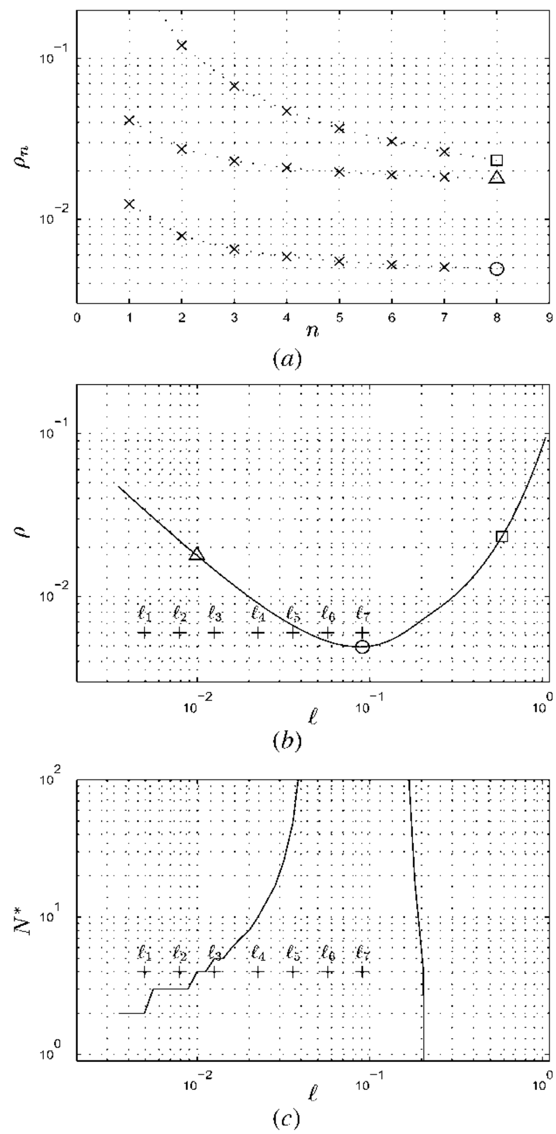

Figure 8. The estimation of the radius of convergence ρ_n is computed for $n \in [1, 8]$ with parameters $\ell = 1e-2$ ($\triangle$), $9.08e-2$ ($\circ$) and 0.6 ($\square$) with $\alpha_0 = 4.77e-1$ $F = 440$ Hz (a). For ($\triangle$) and ($\circ$), ρ_8 yield quite good estimates whereas for ($\square$), ρ_n has not still converged. Similar computations for $\ell \in [1e-3, 1]$ are compiled in (b). As a consequence of (a), $\rho(\ell)$ is a quite good estimation for $\ell < \ell_\circ$ and an significantly overvalued one for $\ell > \ell_\circ$. The amplitude and the lengths ℓ_k used for the simulations of figure 6 are plotted with (+): increasing the order of approximation for ℓ_6 and ℓ_7 will yield asymptotically bad results since the series will diverge in thess cases. In (c), the orders of approximation N^* leading to errors on $q(\ell, \theta)$ similar to that due to the original model (5) are represented. When the remainder of the series R_n is of order a, the corresponding truncated Volterra systems give a coarse representation of the original model. When $R_n = R_{N^*}$ is of order a^2, they give an accurate representation which cannot be improved from the original model point of view. The order of approximation and the lengths ℓ_k used for the simulations in figure 6 are plotted with (+). It clarifies why the simulations performed with $N = 2, 3, 4$ have no qualitative differences for $\ell_{k=1,2,3}$. For the same reasons as in (b), the part $\ell > \ell_\circ$ is underestimated.

- this harmonic appears progressively for $\theta \leq \theta_1$ and slower than the fundamental component; this enlightens the progressive activation of the non-linearity with respect to the amplitude $A(\theta)$.

The heaviness of the algortihm may not be considered as a drawback of the Volterra series representations but only of these algorithms. Boyd has shown that Volterra kernels can be approximated by finite-dimensional non-linear systems which make low-cost simulations possible. This tricky step is not invetigated here but the examination of difficulties, esentially due to the fractional derivative in (5), is discussed below.

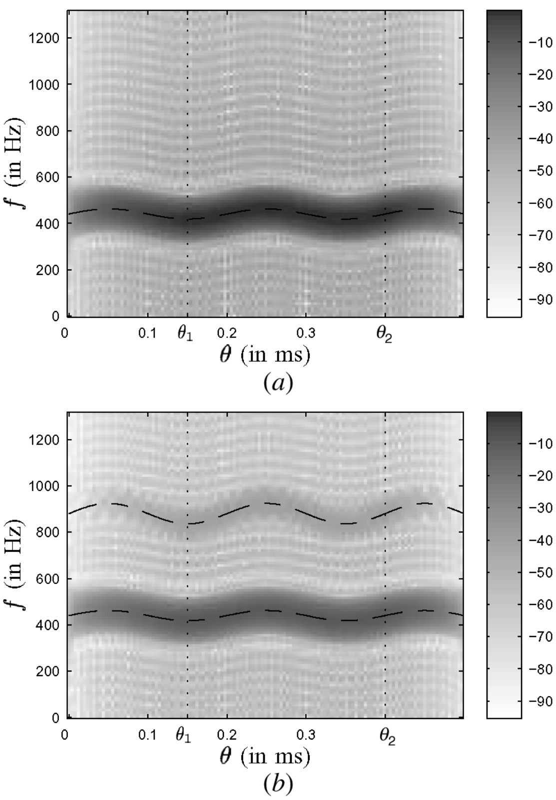

Figure 9. (*a*) Spectrogram of the input $u(\theta)$ and frequency $f(\theta)$ (– –). (*b*) Spectrogram of the output $q(\ell, \theta)$ and frequencies $f(\theta)$, $2f(\theta)$ (– –).

5. Limitations and extensions

5.1. *Limitations*

The complex structure of the kernels in the Laplace domain makes the analytic derivation of inverse Laplace transforms difficult. A first difficulty comes from the square-root of the Laplace variables, due to viscothermal losses, requiring to define the kernels H_n with a cut, namely on $\mathbb{C} \setminus \mathbb{R}^-$. This leads complication in defining a $(n-1)$-dimensional Bromwich contour and applying the residue theorem to derive the inverse Laplace transform. Only the kernel H_1 has the well-known solution (62). The second difficulty is due to the expressions of the functions f_κ, which makes the proof of the convergence of the series difficult. Only a numerical estimation of the radius of convergence has been performed here.

The numerical computation of the output for non-stationary inputs requires a very high amount of floating point operations. A better means would be to build a realization of the system from identification of the kernels (Rugh 1981, chap. 4) and simulate this system. But, the identification of such a realization is not straightforward, once again. The first reason still comes from the pseudo-differential operators such as $\sqrt{s}$ and $e^{-\alpha_0 \ell \sqrt{s}}$, which are associated to infinite dimensional time-realizations (Staffans 1994). The second reason comes from the non-unicity of the Volterra kernels. Identifying a realization from kernels can be performed from the 'regular kernels' (see Rugh 1981, chap. 4) which are not those derived here. Unfortunately, their computation makes difficulties similar to those of inverse Laplace transforms appear.

5.2. *Extensions*

The method presented in (3) with the decomposition (18) can be straightforwardly extended to model with polynomial non-linearity of higher order and for other kind of dampings. Thus, replacing the damping model $-\alpha_0 \sqrt{s}\, \hat{q}(\ell, s)$ by $-\alpha_0\, H(s)\, \hat{q}(\ell, s)$ leads to the same solutions taking $s \mapsto H(s)$ in place of $s \mapsto \sqrt{s}$ to build the functions ϕ_λ.

Replacing the non-linearity $q \partial_\theta q$ by $P[\partial_\theta]\, Q(q)$ where P and Q are polynomials yields a more general sum of crossed products in place of the right hand-side of (32). Building the functions $f_\kappa^{(\ell)}$ and the identification of polynomial coefficients keep a similar recursive law, adapting the sets of indices $\mathcal{K}_n$ and Λ_κ.

Two more general extensions are also quite straightforward for some favorable cases, which are now briefly described. The first one concerns the order of the spatial derivatives. For orders n higher than 1, writing the model as a first-order one for the state $[q, \partial_\ell q, \ldots, \partial_\ell^{n-1} q]$ and the associated boundary conditions can lead to similar resolutions. The second one concerns problems involving several spatial variables for which the system is controlled by a single input. This can be the example of a physical problem for which the active boundary condition is uniform on a surface of control, e.g. pistons for mechanical problems. In this case, the Volterra kernels depend on several space variables and (12) becomes a partial differential equation but it is still linear. If analytic solutions exists for the given boundary conditions, a recursive analytic definition of the kernels can still be achieved.

6. Conclusion

A method to solve analytically a boundary controlled weakly non-linear partial differential equation has been developed, by representing the input/output system for time-varying signals with Volterra series. To the best knowledge of the authors, Volterra series have never been applied in a systematic way to partial differential equations. For the non-linear acoustic propagation model presented here, described by a generalized Burgers' equation, the Volterra kernels has been computed analytically in the Laplace domain (with respect to the time variable). Recursive formula that can readily be implemented on a computer allow us to determine explicitly the Volterra kernels of all orders, yielding an interesting alternative to the recursive calculations by the standard perturbation method e.g. (Schelkunoff 1945, p. 207–209).

When Volterra series are applied to systems described by ordinary differential equations, the kernels in the Laplace domain are determined recursively by solving linear algebraic equations. In the case of partial differential equations, the equations to be solved become differential ones but they are still linear. In the case presented here, they can be solved analytically.

The explicit expressions for the Volterra kernels allow to obtain an analytic resolution of the harmonic balance method, that is used when the input is periodic and quasi-periodic. Usually, this method is only performed numerically. Most important, however, is the fact that the Volterra series representation of the input/output system allows to apply also non-periodic signals. Computations which avoid aliasing have been implemented by carefully controlling the order of approximation of the series and the sampling frequency. The algorithm, however, is computationally very costly.

If the input/output representation system is to be simulated in real time, as e.g. for virtual musical instruments, the kernels have to be approximated by rational functions in the frequency domain in order to arrive at systems that can be described by a finite number of ordinary differential equations that in turn can be described efficiently. The problem with the case treated in this paper is that the solutions of Burgers' equation have a long memory, because the impulse response of the linear part decreases slower than a damped exponential. Previous works on linear systems with this property, however, used the method of so-called diffusive representations successfully, which suggests the extension of the method to weakly non-linear systems represented by Volterra series. All put together would allow to arrive at good quality computationally low-cost realizations of long-memory weakly non-linear systems.

Acknowledgements

This work is a result of a post-doctoral research which has been achieved in the Laboratory of the Nonlinear Systems (LANOS-EPFL). It has been supported by the 2nd Laboratory of Signal Processing of the Swiss Federal Institute of Technology of Lausanne (LTS2-EPFL). The authors wish especially to thank its leader, Pierre Vandergheynst.

References

Abramowitz, M., and Stegun, I. A., 1970, *Handbook of Mathematical Functions* (New York: Dover).

Boyd, S. P., 1985, Volterra series: Engineering fundamentals. PhD thesis, Harvard University.

Hasler, M., 1999, *Phénomènes non linéaires*, École Polytechnique Fédérale de Lausanne.

Menguy, L., and Gilbert, J., 2000, Weakly non-linear gas oscillations in air-filled tubes: solutions and experiment. *Acta Acusitica*, **86**, 798–810.

Nakhla, M. S., and Vlach, J., 1976, A piecewise harmonic balance technique for determination of periodic response of nonlinear systems. *IEEE Transactions on Circuit Theory*, **23**, 85–91.

Rugh, W. J., 1981, *Nonlinear System Theory, The Volterra/Wiener Approach* (Baltimore: The Johns Hopkins University Press).

Schelkunoff, S. A., 1945, *Electromagnetic Waves* (New York: Von Nostrand).

Staffans, O. J., 1994, Well-posedness and stabilizability of a viscoelastic equation in energy space. *Transactions of the American Mathematical Society*, **345**, 527–575.